JOURNAL OF Materials CHEMISTRY

Preparation of SnO_2 nanorods by annealing SnO_2 powder in NaCl flux

Wenzhong Wang,*[a,b] Congkang Xu,[a] Xiaoshu Wang,[c] Yingkai Liu,[a] Yongjie Zhan,[a] Changlin Zheng,[a] Fengqi Song[a] and Guanghou Wang[a,b]

[a]*National Laboratory of Solid State Microstructures & Department of Physics, Nanjing University, Nanjing 210093, People's Republic of China. E-mail: wangqun@nju.edu.cn*
[b]*Structure Research Laboratory, University of Science and Technology of China, Hefei 230026, People's Republic of China*
[c]*Center for Materials Analysis, Nanjing University, Nanjing 210093, People's Republic of China*

Received 8th October 2001, Accepted 19th March 2002
First published as an Advance Article on the web 15th April 2002

SnO_2 nanorods having the rutile structure have been prepared by annealing fine SnO_2 powder in a NaCl flux. The starting SnO_2 powder, the NaCl flux, and surfactant NP9 were mixed and heated at 800 °C for 2.5 h. The nanorods have diameters of *ca.* 20–40 nm and lengths of up to 1 μm. High-resolution transmission electron microscopy (HRTEM), selected area electron diffraction (SAED) and X-ray diffraction (XRD) showed that the nanorods were well-crystallized with a rutile structure. The structure features and chemical composition of the as-prepared nanorods were analyzed by XRD, TEM, HRTEM, SAED, EDS and FTIR. A possible growth mechanism of the nanorods was described by the studies of the formation of nanorods with comparative experiments. The effects of NaCl and NP9 are discussed in detail.

1 Introduction

One-dimensional (1D) nanoscale materials have stimulated great interest recently both because of their unique electronic, optical, and mechanical properties and because of their potential applications in nanodevices.[1,2] Many attempts have been made to synthesize one-dimensional nanostructure materials using a variety of nanofabrication techniques and crystal growth methods, such as arc discharge,[3] laser ablation,[4] template,[5,6] solution,[7–9] and other methods.[10–12] However, to our knowledge, higher temperatures, special conditions, tedious procedures, long synthesis times, complex apparatus or the use of noxious gas compounds may be required for these methods. It has been and still is a challenge to find a novel and simple synthetic route for one-dimensional nano-scale materials.

Semiconductor one-dimensional nano-sized materials are known to have many interesting physical properties and great applications in optoelectronic devices, solar energy conversion, nonlinear optical, photoelectrochemical cells and heterogeneous photocatalysis.[13,14] The rutile form of SnO_2 is one of the important materials. It is an n-type semiconductor with a large band gap, and is well-known for its applications in gas sensors,[15,16] dye-based solar cells,[17] transistors,[18] electrode materials,[19] catalysts,[20] and opticalconductive films for solar cells,[21] In recent years, attention has been focused on its possible applications in electrochromic devices.[22]

SnO_2 has been synthesized by many methods, such as sol–gel,[23,24] chemical vapor deposition,[25] magnetron sputtering,[26] and evaporation of elemental tin in an oxygen atmosphere,[27] *etc.* However, only SnO_2 particles or films were prepared by these methods.

In this paper, we report a simple route for the preparation of SnO_2 nanorods. SnO_2 nanorods are synthesized by annealing precursor SnO_2 powder in the NaCl flux. The as-prepared nanorods are *ca.* 20–40 nm in diameter and up to 1 μm in length. The nanorods are characterized by XRD, TEM, HRTEM, SAED, EDS, and FTIR. The growth mechanism of SnO_2 nanorods and the effects of NaCl and NP9 in the formation of nanorods are discussed in detail.

2 Experimental

2.1 Materials

SnO_2 (>99.5%), NaCl (>99.5%), nonyl phenyl ether (NP9) (>99.0%).

2.2 Synthesis of SnO_2 nanorods

0.5 g of starting SnO_2 powder was mixed with 1.5 g of NaCl and 4 ml of NP9 using an agate mortar and then the mixture was ground for 30 min by hand. The mixed sample was heated in a porcelain crucible that was placed in the middle of an alumina tube with a horizontal tube electric furnace at 800 °C for 2.5 h, the heat treatment sample was then cooled gradually to room temperature in air, washed several times with distilled water to remove the NaCl flux, filtered, and then dried in an oven at 70 °C for 3 h. The obtained products were collected for characterization by XRD, TEM, HRTEM, SAED, EDS and FTIR.

2.3 Equipment

X-Ray powder diffraction (XRD) patterns were obtained on a Japan Rigaku D_{Max} γ_A X-ray diffractometer with Cu-Kα radiation (λ = 0.154178 nm), employing a scanning rate of 0.02° s^{-1} in the 2θ range from 20–80°. Transmission electron microscopy (TEM) images and selected area electron diffraction (SAED) patterns were taken with a JEM-200 CX transmission electron microscope, using an accelerating voltage of 200 kV. The samples for these measurements were dispersed in absolute ethanol with an ultrasonic generator, and then the solutions were dropped onto copper grids coated with amorphous carbon films. High-resolution transmission electron microscopy (HRTEM) and energy-dispersive X-ray

 DOI: 10.1039/b109130c

spectroscopy (EDS) were carried out on a JEOL-2010 electron microscope, using an accelerating voltage of 200 kV. Infrared spectra were recorded using a Nicolet 170 SX Fourier transform infrared spectroscopy (FTIR) spectrometer from 4000 to 400 cm^{-1} at room temperature. The samples and KBr crystals were ground together, and the mixture was pressed into a disc for recording the spectrum. The 514.5 nm line of the laser was the excitation source, with the capability of supplying 30 mW power.

3 Resuts and discussion

3.1 Characterization of SnO_2 nanorods

To characterize the structural features and chemical composition of the nanorods, investigations of XRD, TEM, HRTEM, SAED, EDS, and FTIR were carried out on these nanorods.

Phase identification of as-prepared nanorods was carried out using the XRD pattern shown in Fig. 1. All diffraction peaks can be perfectly indexed with respect to the rutile SnO_2 structure, not only in peak position, but also in their relative intensity. XRD patterns showed that the materials were SnO_2 with the refined lattice parameters. The average SnO_2 lattice constants obtained by refinement of the XRD data for the as-synthesized samples are $a = 4.732$ Å and $c = 3.184$ Å, which are consistent with those of bulk SnO_2 (JCPDS 21-1250).

The morphology of the nanorods was observed by TEM. A typical TEM image of the as-synthesized nanorods is shown in Fig. 2a. It can be seen that SnO_2 crystals display a rod-like shape with a diameter of 20–40 nm and length of up to 1 μm. We also find that these nanorods are relatively straight and their surfaces are smooth, and that there are no spherical droplets at their tips. Fig. 2b shows a typical SAED pattern, which confirms that the nanorods are the single crystal rutile SnO_2.

HRTEM is a powerful method for structural analysis on the atomic scale, and thus might provide further insight into the structure of an individual SnO_2 nanorod. Fig. 2c shows an HRTEM image of the as-prepared nanorods. The image shows that SnO_2 nanorods are structurally uniform and single crystalline with no defects and dislocations; the interplanar spacing is *ca.* 0.343 nm, which corresponds to the (110) plane of the rutile crystalline SnO_2. The chemical composition analysis by EDS from a local area shows that the nanorods are composed of only Sn and O. Further quantitative analysis reveals that the atomic ratio of Sn : O is 32.75 : 67.25, which is *ca.* 1 : 2.

Fig. 3 shows the FTIR spectrum of the nanorods. Here, the two characteristic absorption peaks, at 675.3 and 476.8 cm^{-1}, can be attributed to the SnO_2.[28] We find no other peaks in the spectrum. The peak at 675.3 cm^{-1} is assigned to the anti-symmetric Sn–O–Sn stretching mode of the surface-bridging oxide formed by condensation of an adjacent hydroxy group; the peak at 476.8 cm^{-1} is assigned to a symmetric Sn–O–Sn stretching mode. Thus the IR spectrum further confirms that the sample is composed of SnO_2.

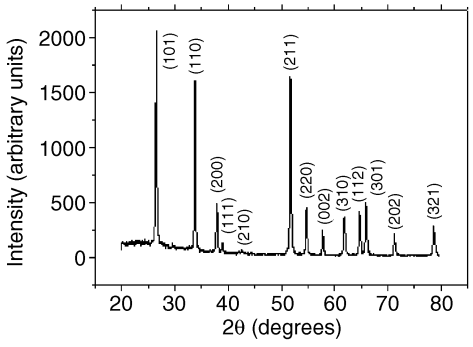

Fig. 1 X-Ray diffraction pattern of the as-prepared SnO_2 nanorods.

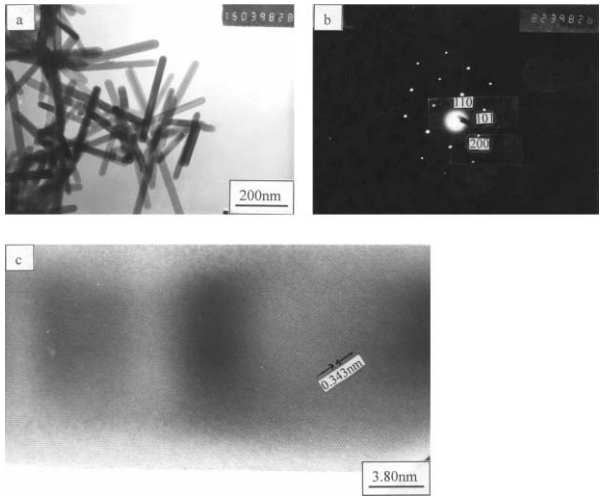

Fig. 2 (a) TEM image of SnO_2 nanorods; (b) SAED pattern of SnO_2 nanorods; (c) HRTEM image of a 20 nm SnO_2 nanorod.

3.2 Growth mechanism of the nanorods

Nanorods synthesized *via* this annealing process are regular with a relatively straight, rod-like shape. Moreover, there are no spherical liquid droplets at the tips of the nanorods, which are known to be good evidence for the vapor–liquid–solid (VLS)[29] and solution–liquid–solid (SLS)[7] mechanisms. This suggests that the nanorods formed *via* our method may not grow by the VLS or SLS mechanisms. In order to reveal further the growth mechanism and the effects of NaCl and the surfactant NP9, we performed the following comparative experiments at the same synthesis conditions (the same heating temperature, quantity of each starting material, soaking and grinding times): (a) adding NaCl and NP9, gradually cooling to room temperature (5 °C min^{-1}); (b) adding NaCl and NP9, quickly cooling to room temperature (40 °C min^{-1}); (c) adding only NaCl; (d) adding only NP9; (e) no addition of NaCl and NP9. We obtained following experimental results: (1) only experiments (a) and (b) can form nanorods, which are shown in Figs. 4a and b, and the other three experiments cannot form

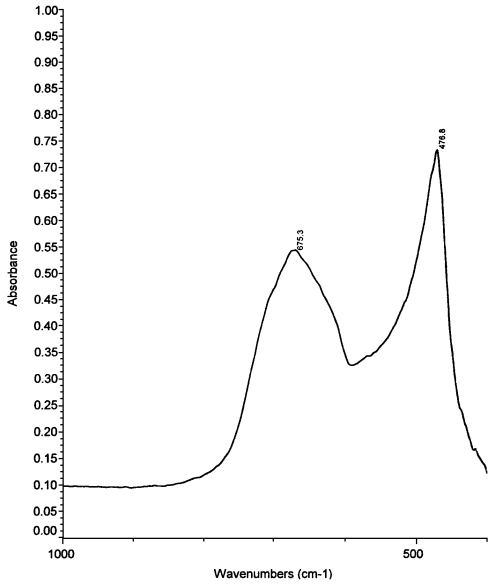

Fig. 3 FTIR spectrum of the as-prepared SnO_2 nanorods.

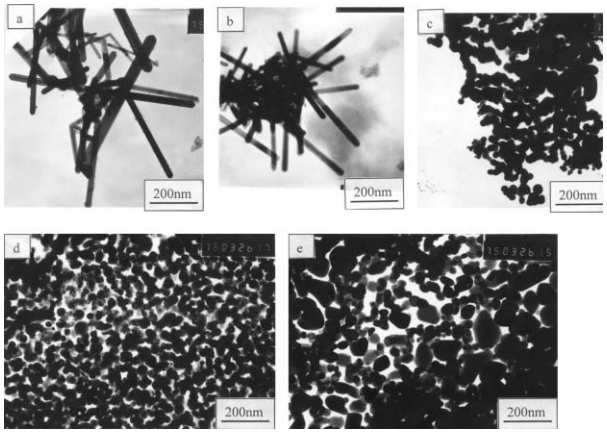

Fig. 4 (a) TEM images of SnO_2 nanorods prepared by adding NaCl and NP9, and gradually cooling to room temperature; (b) TEM images of SnO_2 nanorods prepared by adding NaCl and NP9, and quickly cooling to room temperature; (c) TEM images of SnO_2 particles prepared from adding only NaCl; (d) TEM images of SnO_2 particles prepared from adding only NP9; (e) TEM images of SnO_2 particles prepared by no addition of NaCl and NP9.

nanorods but produce only nanoparticles, which are shown in Figs. 4c–e; (2) the average length and diameter of the nanorods did not show a clear dependence on the cooling rate. These results indicate that the growth mechanism of the nanorods in this route is different with that in the usual 'flux method' in which the product crystals are obtained during the cooling process.[30] That is, the nanorods formed *via* the present method grow not during the cooling process, but during the soaking of the melt. This suggests that the nanorods formed *via* our method may grow mainly by an Ostwald ripening mechanism, *i.e.* the dissolving of fine particles and the deposition of components on larger particles.

3.3 Effects of NaCl and surfactant NP9

When Ostwald ripening is the dominant mechanism of nanorod growth, the formation of the nanorods must be affected by the character of the starting material, such as the particle size and/or chemical activity, because the dissolution rate of the material depends on such characters. The viscosity of the flux during heating of the system also affects the formation of nanorods,[31] and these points can be confirmed by the above-mentioned experiments. In these experiments, only (a) and (b) can form nanorods (Figs. 4a, b), whereas experiments (c), (d) and (e) all produce nanoparticles (Figs. 4c–e). These results may give an explanation of the effects of NaCl and NP9 in the formation of nanorods. Since adding NaCl can significantly decrease the viscosity of the melt,[31] this makes the mobility of components in the flux easier. So, adding NaCl can provide a favorable environment for the growth of nanorods. The surfactant NP9 may play the following role: during the grinding process of the precursor SnO_2 particles, adding the NP9 is favorable to the formation of fine particles because the NP9 may form a 'shell' surrounding the particles to prevent them from aggregating to larger particles, thus decreasing the size of the precursor SnO_2 particles. Fig. 5a shows the TEM image of ground precursor SnO_2 particles. The average diameter of as-ground SnO_2 particles is *ca.* 100 nm, but most particles with a diameter of less than 100 nm can also be found. These particles display an irregular shape. Fig. 5b shows TEM images of SnO_2 particles before grinding. It can be seen that the average diameter of the unground SnO_2 particles is *ca.* 150 nm. Some particles with a diameter of more than 300 nm can be found. The unground SnO_2 particles also have an irregular form. Consequently, ground precursor powders have highly-specific surfaces and are metastable in the annealing process, which makes it easy to further fabricate nanorods. This is also

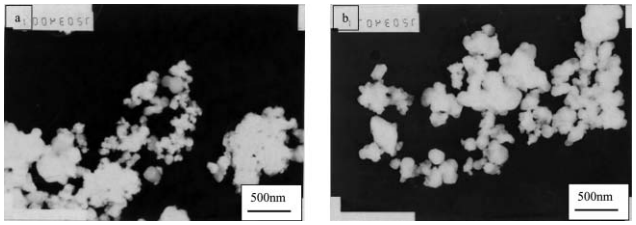

Fig. 5 TEM images of (a) ground precursor SnO_2 particles; (b) SnO_2 particles before grinding.

favorable for the formation of nanorods. That is why the nanorods can grow only in (a) and (b) experiments, but not in the cases (c), (d) and (e).

4 Conclusions

A simple annealing process has been successfully developed to synthesize SnO_2 nanorods. These nanorods have a diameter of 20–40 nm and length of up to 1 μm. The structural nature and chemical composition of the nanorods were analyzed by XRD, TEM, HRTEM, EDS and FTIR. In comparison to the mechanism of some other methods for the fabrication of one-dimensional nano-scale materials, the formation mechanism of nanorods by our method is different. We propose that the nanorods prepared using this method might fabricate mainly by an Ostwald ripening mechanism. This method is simple and controllable, and thus, the product SnO_2 nanorods can be of high purity.

Acknowledgements

This work was supported by the National Nature Science Foundation of China (Nos. 29890210, 10023001, 10074024).

References

1 J. R. Heath, P. J. Kuekes, G. Synder and R. S. Williams, *Science*, 1998, **280**, 717.
2 C. M. Lieber, *Solid State Commun.*, 1998, **107**, 607.
3 S. Iijima, *Nature*, 1991, **354**, 56.
4 A. Thess, R. Lee, P. Nikolave, H. Dai, P. Petit, J. Robert, C. H. Xu, Y. H. Lee, S. G. Kim, A. G. Rinzler, D. T. Colbert, G. E. Scuseria, D. Tomanek, J. E. Fisher and R. E. Smalley, *Science*, 1999, **271**, 483.
5 C. R. Martin, *Science*, 1994, **266**, 1961.
6 B. R. Martin, D. J. Dermody, B. D. Reiss, M. M. Fang, L. A. Lyon, M. J. Natan and T. E. Mallouk, *Adv. Mater.*, 1999, **11**, 1021.
7 T. J. Trentler, K. M. Hickman, S. C. Goel, A. M. Viano, P. C. Gibbons and W. E. Buhro, *Science*, 1995, **270**, 1791.
8 Y. Li, Y. Ding and Z. Wang, *Adv. Mater.*, 1999, **11**, 847.
9 J. D. Hopwood and S. Mann, *Chem. Mater.*, 1997, **9**, 1819.
10 Z. W. Pan, Z. R. Dai and Z. L. Wang, *Science*, 2001, **291**, 1947.
11 Z. G. Bai, D. P. Yu, H. Z. Zhang, Y. Ding, Y. P. Wang, X. Z. Gai, Q. L. Hang, G. C. Xiong and S. Q. Feng, *Chem. Phys. Lett.*, 1999, **303**, 311.
12 P. Yang and C. M. Lieber, *Science*, 1996, **273**, 1836.
13 K. Hu, M. Brust and A. Bard, *Chem. Mater.*, 1998, **10**, 1160.
14 C. B. Murray, C. R. Kagan and M. G. Bawendi, *Science*, 1995, **270**, 1335.
15 G. Ansari, D. Boroojerdian, S. R. Sainker, R. N. Karekar, R. C. Aiyer and S. K. Kulkarni, *Thin Solid Films*, 1997, **295**, 271.
16 P. G. Harrison and M. J. Willet, *Nature*, 1988, **332**, 337.
17 S. Ferrere, A. Zaban and B. A. Gsegg, *J. Phys. Chem. B*, 1997, **101**, 4490.
18 A. Aoki and H. Sasakura, *Jpn. J. Appl. Phys.*, 1970, **9**, 582.
19 J. J. Rowlette and H. I. Attia, *Proc. Electrochem. Soc.*, 1987, 7.
20 S. R. Stampfl, Y. Chen, J. A. Dumesis, Ch. Niu and C. G. Hill, *J. Catal.*, 1987, **105**, 445.
21 C. Agashe, M. G. Takwale, B. R. Marathe and V. G. Bhide, *Sol. Energy Mater.*, 1988, **17**, 99.
22 P. Olivi, E. C. Pereira, E. Longo, J. A. Varella and L. O. D. S. Bulhoes, *J. Electrochem. Soc.*, 1993, **140**, L81.

23 D. Wang, S. Wen, J. Chen, S. Zhang and F. Li, *Phys. Rev. B*, 1994, **49**, 14 282.
24 A. Maddalena, R. Del Maschio, S. Dire and A. Raccanelli, *J. Non-Cryst. Solids*, 1990, **121**, 365.
25 R. D. Tarey and T. A. Raju, *Thin Solid Films*, 1995, **128**, 181.
26 T. Minami, H. Nanto and S. Takata, *Jpn. J. Appl. Phys.*, 1988, **27**, L287.
27 V. Schlosser and G. Wind, in *Proceedings of the 8th EC Photovoltaic Solar Energy Conference*, Florence, Italy, 1998, p 998.
28 P. G. Harrison, N. C. Lloyd, W. Daniell, C. Bailey and W. Azelee, *Chem. Mater.*, 1999, **11**, 896.
29 R. S. Wagner and W. C. Ellis, *Appl. Phys. Lett.*, 1964, **4**, 89.
30 S. Hayashi, M. Sugai, Z. Nakagawa, T. Takei, K. Kawasaki, T. Katsuyama, A. Yasumori and K. Okada, *J. Eur. Ceram. Soc.*, 2000, **20**, 1099.
31 Y. T. Chen, J. B. Li, Q. M. Wei and H. Z. Zhai, *J. Cryst. Growth*, 2001, 224.